$(\alpha,\alpha p)$ quasifree proton knockout reaction on ^{2}H, ^{6}Li, and ^{19}F

A. Nadasen, T. A. Carey, P. G. Roos, N. S. Chant, C. W. Wang,* and H. L. Chen
Department of Physics and Astronomy, University of Maryland, College Park, Maryland 20742
(Received 9 February 1979)

The $(\alpha,\alpha p)$ reaction on ^{2}H, ^{6}Li, and ^{19}F has been studied with 140 MeV α particles. Energy spectra for the ground state transition are presented at one angle pair for ^{2}H and ^{19}F, and three angle pairs for ^{6}Li. Distorted-wave impulse-approximation calculations provide good fits to the ^{2}H data, the ^{19}F data, and data at one angle pair for ^{6}Li. The other two angle pairs for ^{6}Li show significant deviations from the distorted-wave impulse-approximation suggesting contributions from processes more complicated than those included in the distorted-wave impulse-approximation.

[NUCLEAR REACTIONS ^{2}H, ^{6}Li, $^{19}F(\alpha,\alpha p)$, $E_\alpha = 140$ MeV; measured $(E_p, E_\alpha, \theta_p, \theta_\alpha)$; DWIA analysis; deduced spectroscopic factors.]

I. INTRODUCTION

Quasifree proton knockout reactions can provide important information on the single particle structure of nuclei. A number of $(p,2p)$ reactions performed at medium energies have provided information on the location of the single particle strength of deep-lying shells and at least qualitative information on the single particle wave function.[1-3] The (e,ep) reaction, although more difficult to study experimentally, has the advantage that the electrons are more penetrating in addition to the fact that the electron-proton interaction is well understood. Such studies[4,5] thus provide information on deeper-lying single particle states as well as more quantitative information on the single particle wave function, particularly at small radii.

In contrast, owing to the strong absorption of the α particles, we expect the $(\alpha,\alpha p)$ reaction to be very surface localized in comparison to the (e,ep) and $(p,2p)$ reactions. Thus it offers the possibility of studying the single particle wave functions of valence nucleons at large radii where the wave function is determined by the spectroscopic factor and the binding energy tail.

Very few experimental studies of the $(\alpha,\alpha p)$ reaction have been performed. Thus, before extracting nuclear structure information, one must first demonstrate that the distorted-wave impulse-approximation (DWIA)[6] assuming a quasifree reaction mechanism is applicable under the chosen experimental conditions.

As an initial investigation we have measured the $(\alpha,\alpha p)$ reaction with 140 MeV incident α particles on targets of ^{2}H, ^{6}Li, and ^{19}F. The ^{2}H target was chosen primarily for setup purposes, but it does provide some information on the reaction mechanism. The main interest in the ^{6}Li target is that the transition to the ground state of ^{5}He permits both s and p wave proton knockout, due to the fact that the final state is unbound.[7] A DWIA analysis of the $^{6}Li(p,2p)^{5}He$ reaction shows that the relative s and p contributions depend upon distortion effects,[8] so a comparison of the $(\alpha,\alpha p)$ and $(p,2p)$ reactions should provide more insight into these reactions. Finally, ^{19}F was chosen as a heavier target primarily due to the fact that the ground state transition is pure $l=0$, thereby enhancing the knockout cross section.

In the following we discuss the experimental details (Sec. II) and the DWIA analysis of the $(\alpha,\alpha p)$ reaction (Sec. III) and finally we compare this reaction to other knockout reactions (Sec. IV).

II. EXPERIMENT AND RESULTS

A. Experimental Details

A 140 MeV α-particle beam from the University of Maryland Isochronous Cyclotron was energy analyzed to approximately 90 keV and focused at the center of a 1.5 m diameter precision scattering chamber. The outgoing particles were detected with two counter telescopes placed coplanar with, and on opposite sides of, the beam. The α-particle detector telescope consisted of a 300 μm Si surface barrier ΔE detector followed by a 5 mm Si (Li) E detector rotated by 45° (effective thickness of approximately 7 mm). The solid angle of this telescope was 0.31 msr (approximately $1° \times 1°$). The proton detector telescope consisted of a 1000 μm Si surface barrier ΔE detector followed by a 5 cm thick, 2.5 cm diameter cylindrical NaI(Tl) crystal E detector. The solid angle of the proton telescope was 4.65 msr.

A fast signal from each detector was used to form $\Delta E \cdot E$ coincidences for each telescope with a resolving time less than the time between adjacent rf beam bursts. The outputs of these two $\Delta E \cdot E$ coincidence units, their relative timing determined by the ΔE signals, were used as start and stop signals for a time-to-amplitude converter (TAC), thus allowing simultaneous storage of real and accidental coincidence events. The time resolution for α-p coincidence events was better than 3 ns.

The slow linear signals were handled with conventional electronics. The five linear signals (ΔE_α, E_α, ΔE_p, E_p, and TAC), suitably gated by coincidence requirements, were sent to analog-to-digital converters interfaced with an IBM 360/44 computer. The data were analyzed on-line as well as written event-by-event on magnetic tape for subsequent analysis. Particle identification and various gating requirements were performed by computer software. Dead time corrections were made using a four channel pulser triggered by the Faraday cup scaler.

The targets consisted of a deuterated polyethylene foil (0.3 mg cm^{-2} of ^{2}H), a rolled ^{6}Li (99%) foil 3.3 mg cm^{-2} thick transferred to the scattering chamber under vacuum to prevent oxidation, and a Teflon $(C_2F_4)_n$ foil providing a 2.03 mg cm^{-2} thick ^{19}F target. Owing to deterioration of the Teflon foil under beam, this target was constantly monitored and moved when necessary.

Coincident α-p data were obtained only at quasifree angle pairs, i.e., angle pairs for which it is kinematically possible for the residual undetected nucleus to be left at rest, in order to enhance the importance of the quasifree knockout mechanism. Energy sharing data were obtained at one angle pair for ^{2}H and ^{19}F and at three angle pairs for ^{6}Li. The overall residual nucleus binding energy resolution of the two telescope system was approximately 500 keV as measured using ^{1}H$(\alpha, \alpha)^1$H free α-p coincidences. (The binding energy B, defined by $T_0 - B = T_\alpha + T_p + T_3$, where T_0 is the projectile kinetic energy, T_α and T_p are the detected particle kinetic energies, and T_3 is the computed kinetic energy of the recoiling residual nucleus, determines the resolution in residual nucleus excitation energy.)

B. Experimental Results

The binding energy spectrum for ^{19}F is shown in Fig. 1. In addition to the ^{19}F$(\alpha, \alpha p)^{18}$O ground state transition we observed peaks associated with transitions to excited states of ^{18}O, as well as the ground and excited states of ^{11}B from the ^{12}C in the Teflon target. The binding energy spectra from the ^{6}Li$(\alpha, \alpha p)^5$He reaction at two angle pairs are

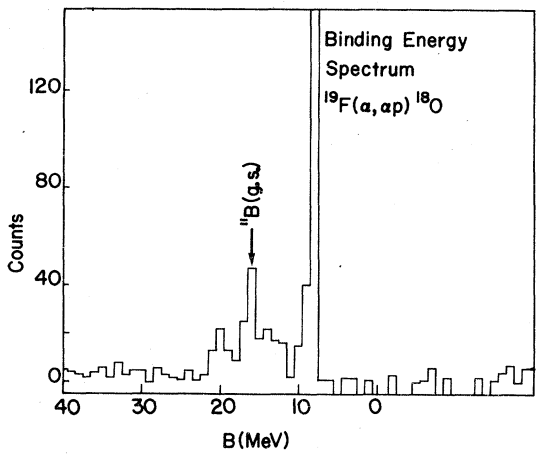

FIG. 1. The binding energy spectrum for ^{19}F$(\alpha, \alpha p)^{18}$O at $E_\alpha = 140$ MeV.

presented in Fig. 2. We observed strong transitions to the ^{5}He ground state at all three angle pairs studied, but only the $\theta_\alpha/\theta_p = 12.5°/-27.0°$ angle pair shows significant excitation of excited states near 20 MeV, which presumably arise from $1s_{1/2}$ proton removal.

The energy sharing spectrum for ^{2}H$(\alpha, \alpha p)n$ is shown in Fig. 3. The cross section peaks at an α energy corresponding to leaving the residual neutron at rest, which is consistent with the knockout of an s-state proton. This distribution is also narrower than those for the other targets studied, reflecting the fact that the wave function of the proton in deuterium is relatively weaker in high momentum components.

The energy sharing spectrum for the ^{19}F$(\alpha, \alpha p)$-^{18}O ground state transition ($\frac{1}{2}+ \rightarrow 0+$) is shown in Fig. 4. Again the cross section peaks near zero recoil momentum as would be expected for the knockout of the $2s_{1/2}$ proton.

In Fig. 5 we present the energy sharing spectra for the three angle pairs measured in the ^{6}Li$(\alpha, \alpha p)^5$He reaction. In each case these data represent a sum over 3 MeV bin in binding energy centered about the ground state ($\frac{3}{2}^-$) n-α resonance in the corresponding binding energy spectrum. The data for the $10.0°/-55.2°$ angle pair show a very slight minimum near zero recoil momentum, suggesting the presence of both p-state and s-state knockout, as observed for the ^{6}Li$(p, 2p)^5$He reaction. At $12.0°/-47.5°$ the data show a definite asymmetry about $p_3 = 0$, as well as a reduced cross section at $p_3 = 0$. This asymmetry becomes even more pronounced for the angle pair $12.5°/-27.0°$. At this angle pair, which corresponds to the second solution in free α-p kinematics, we obtain a significantly enhanced yield on the high α energy

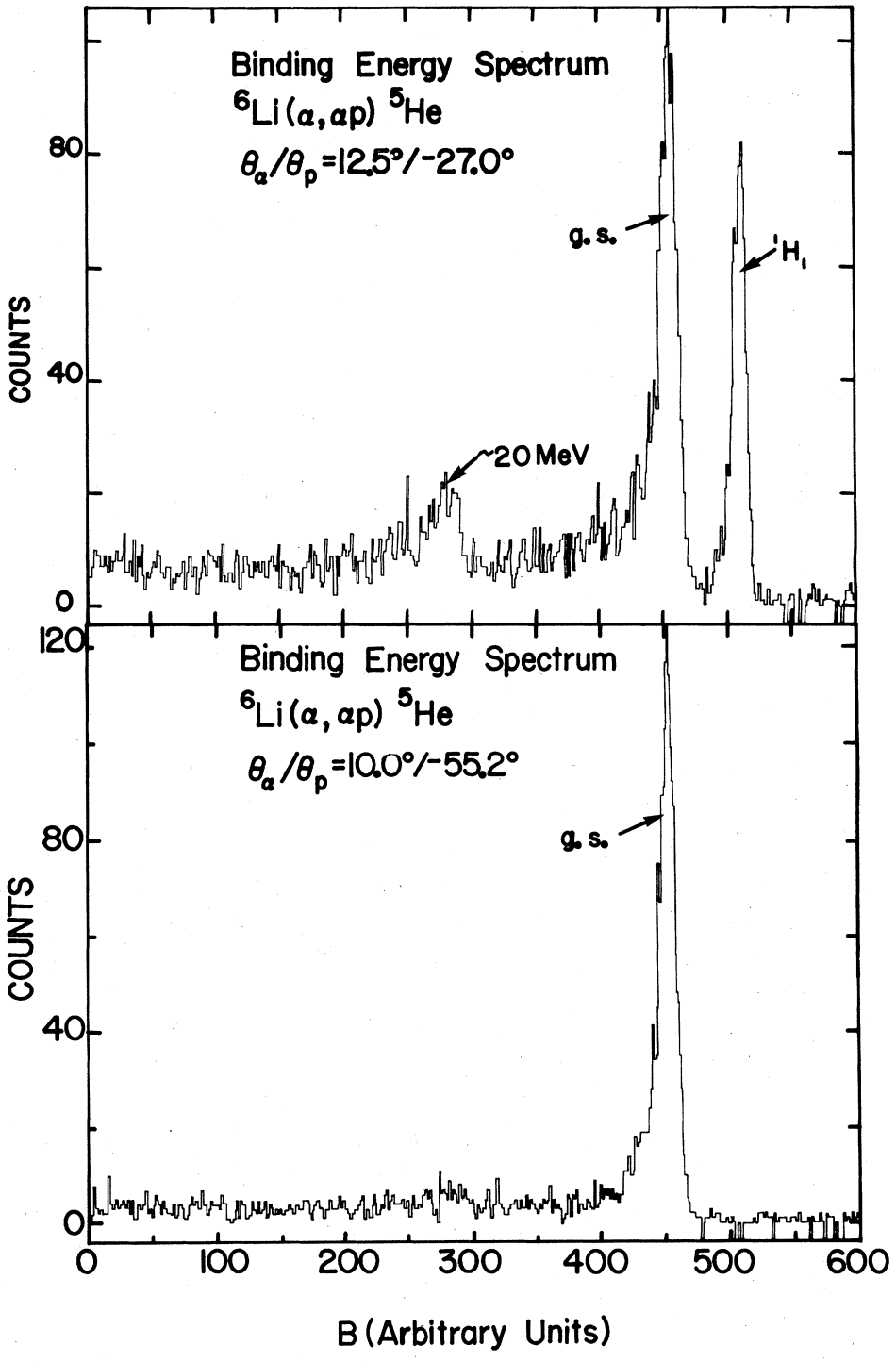

FIG. 2. The binding energy spectra for ^{6}Li($\alpha, \alpha p$)^{5}He at E_α = 140 MeV, for angle pairs (a) $\theta_\alpha | \theta_p$ = 12.5°/− 27.0° and (b) $\theta_\alpha | \theta_p$ = 10.0°/− 55.2°.

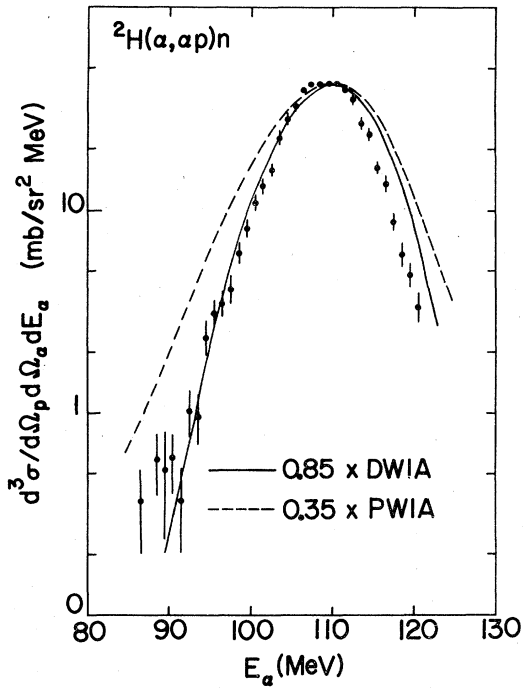

FIG. 3. The energy sharing spectrum for ^{2}H($\alpha, \alpha p$)n. The dashed curve is a PWIA calculation (normalized by 0.35) and the solid curve is a DWIA calculation (normalized by 0.85).

side of the distribution. Also the cross section at $p_3 = 0$ is reduced compared to the other two angle pairs.

III. ANALYSIS

The analysis of these data was carried out with the distorted-wave impulse-approximation (DWIA). In the DWIA the $A(\alpha, \alpha p)B$ knockout cross section

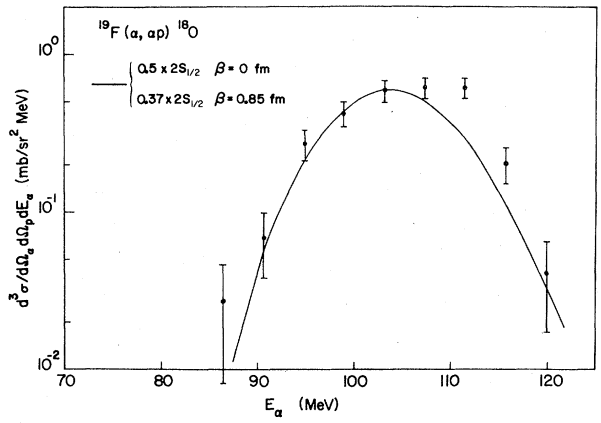

FIG. 4. The energy sharing spectrum for the ^{19}F(α, αp)^{18}O(0+, g.s.) reaction. The curve represents DWIA calculations for the knockout of a $2s_{1/2}$ proton normalized to the data by the factors indicated.

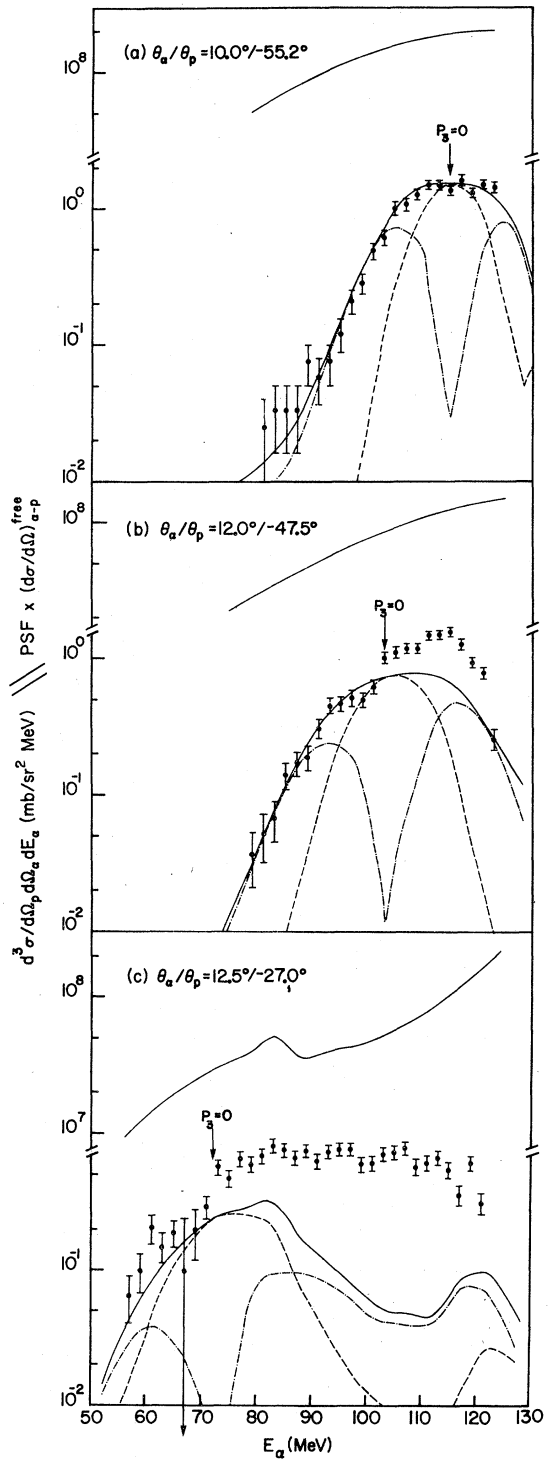

FIG. 5. The energy sharing spectra for the ^{6}Li(α, αp)^{5}He ground state transitions at three angle pairs. The upper curve in each spectrum shows the variation of the product $(KF \times d\sigma/d\Omega|_{\alpha-p})$. The dashed curves represent $2s_{1/2}$ DWIA calculations (normalized by 0.1) and the dot-dashed curves represent $1p_{3/2}$ calculations (normalized by 0.7). The solid lines represent the sum of the two calculations.

can be written in the form[6]

$$\frac{d^3\sigma}{d\Omega_p d\Omega_\alpha dE_\alpha} = C^2S \times KF \times \frac{d\sigma}{d\Omega}\Big|_{\alpha-p} \times \sum_\Lambda |T_L^\Lambda|^2 ,$$

where C^2S is the usual single particle spectroscopic factor, KF is a known kinematic factor, and $d\sigma/d\Omega|_{\alpha-p}$ is the two-body α-p cross section. The quantity T_L^Λ is given by

$$T_L^\Lambda = (2L+1)^{-1/2} \int \chi_p^{(-)*}(\vec{r})\chi_\alpha^{(-)*}(\vec{r})\phi_L^\Lambda(\vec{r})\chi^{(+)}\left(\frac{B}{A}\vec{r}\right) d^3r ,$$

where the χ's are distorted waves for the incoming and outgoing particles and $\phi_L^\Lambda(\vec{r})$ is the bound proton wave function. In the plane wave limit (PWIA) T_L^Λ represents the momentum space wave function for the bound proton.

The DWIA calculations were carried out with the code THREEDEE written by Chant. The distorted waves were calculated from Woods-Saxon potentials obtained via elastic scattering analyses. Except in the case of deuterium, the bound proton wave function was calculated by binding the particle in a Woods-Saxon potential including a spin-orbit term, with the depth of the central potential chosen to reproduce the proton separation energy. The two-body cross section $d\sigma/d\Omega|_{\alpha-p}$, which is properly evaluated half-off the energy shell, was typically replaced by the α-p on-shell cross section corresponding to the measured final state of the α-p pair (final energy prescription). However, other possible choices were also investigated.

As expected, based on DWIA analyses of other types of knockout reactions,[6] the inclusion of distortion effects is found to be crucial. For the cases studied here, the magnitude of the DWIA cross section at $p_3 = 0$ is reduced when compared to the PWIA calculations by factors ranging approximately from 2.5 to 40, depending on the target. Additionally, the shape of the energy sharing spectrum is generally significantly modified by the distortion effects.

A. ^{2}H$(\alpha,\alpha p)n$

Calculations for $^2\mathrm{H}(\alpha,\alpha p)n$ were carried out using a Hulthén wave function for the deuteron in all cases. The dashed curve in Fig. 3 shows the resulting PWIA calculation normalized to the experimental data. The importance of multiple scattering effects is clear both in terms of magnitude (the PWIA calculation is a factor of 3 too large) and shape. These results are rather similar to those obtained for $^2\mathrm{H}(\alpha,\alpha p)n$ at 78 MeV by Bonbright,[9] suggesting that there is no large decrease in multiple scattering effects with an increase of almost a factor of 2 in bombarding energy.

Although the application of the DWIA to such light systems may be questionable, we have performed calculations to investigate the ability of the DWIA to correct the major discrepancies observed in the PWIA calculation. The entrance channel optical potential was obtained from α-d elastic scattering.[10] For the exit channel, $\chi_\alpha^{(-)}$ was calculated with an optical potential obtained from an analysis of p-α elastic scattering[11] while $\chi_p^{(-)}$ was determined from either a real nucleon-nucleon potential or no potential at all (plane wave). Turning off the p-n interaction in the exit channel affects the magnitude of the result by only 10% with no significant change in shape.

The resultant DWIA calculation is represented by the solid line in Fig. 3, again normalized to the experimental data. The normalization constant is 0.85, which shows that the inclusion of distortion effects removes most of the discrepancy observed in the PWIA. The agreement in shape is also significantly improved, with some of the remaining discrepancies being perhaps due to the approximate treatment of recoil effects in the DWIA. However, for such a light target the overall agreement between the DWIA and the experiment is remarkably good.

B. ^{19}F$(\alpha,\alpha p)^{18}$O (0+, ground state)

Calculations for the $^{19}\mathrm{F}(\alpha,\alpha p)^{18}\mathrm{O}$ ground state ($\frac{1}{2}+ \rightarrow 0+$ transition) were carried out assuming the knockout of a $2s_{1/2}$ proton. The geometry of the Woods-Saxon potential for the bound proton obtained by interpolating the results of Elton and Swift[12] (which reproduce electron scattering and single particle energies) yields the values $r_0 = 1.4$ fm and $a = 0.6$ fm. The optical potentials were taken from elastic scattering analyses of $\alpha + {}^{12}$C at 140 MeV (Ref. 13) for the entrance channel and of $\alpha + {}^{12}$C at 104 MeV (Ref. 13) and $p + {}^{16}$O at 30 MeV (Ref. 14) for the exit channel.

The resultant calculations normalized to the experimental energy sharing data are shown as a solid line in Fig. 4. The agreement in shape is quite satisfactory. The normalization gives a spectroscopic factor $C^2S = 0.5$ which is larger than the value 0.38 obtained by Kaschl *et al.*,[15] in an analysis of the $(d, {}^3\mathrm{He})$ reaction at 52 MeV and the value 0.36 obtained by shell-model calculations.[16] However, our result is similar to that obtained by High *et al.*,[17] in a DWIA analysis of the $^{19}\mathrm{F}(p,2p)^{18}\mathrm{O}$ reaction at 42.7 MeV.

A calculation including nonlocality in the bound state with a nonlocality range[18] 0.85 fm was then performed. The effect of the nonlocality correction for the bound state is to increase the DWIA cross section with no change in shape, thus reducing the spectroscopic factor to 0.37, in rather good agree-

ment with the theoretical calculations. The inclusion of nonlocality in the optical channels had a negligible effect due to the strong surface localization of the reaction.

The sensitivity of the calculation to the optical potentials was studied by repeating the DWIA calculations with α potentials obtained from an energy dependent analysis[19] of $\alpha + {}^{24}$Mg. The results differ by only 5% in magnitude, again with no change in shape. Also the effects of choices for $d\sigma/d\Omega|_{\alpha-p}$ other then the final energy prescription were investigated. It was found that the common prescriptions, such as the initial energy prescription, only serve to increase the spectroscopic factor.

Overall, the agreement between the DWIA and experiment is reasonably good. The shape of the energy sharing spectrum is well reproduced, but the magnitude of the spectroscopic factor is somewhat large unless a nonlocal bound state is included. However, the spectroscopic factor is sensitive to both the two-body cross section prescription and the bound state geometry.

The region of sensitivity of the cross section has been studied by calculating the DWIA cross section at $p_3 = 0$ for a series of cutoff radii. The resultant differences in cross section between the various cutoff radii are presented as a function of radius in Fig. 6. From this plot we see that the reaction is very strongly surface localized, the main contributions coming from the region around 6.5 fm. Thus, as discussed in the Introduction, the $(\alpha, \alpha p)$ cross section results from the asymptotic tail of the single particle wave function. This result explains the insensitivity of the shape of the energy sharing distribution to the choice of bound state geometries and optical potentials.

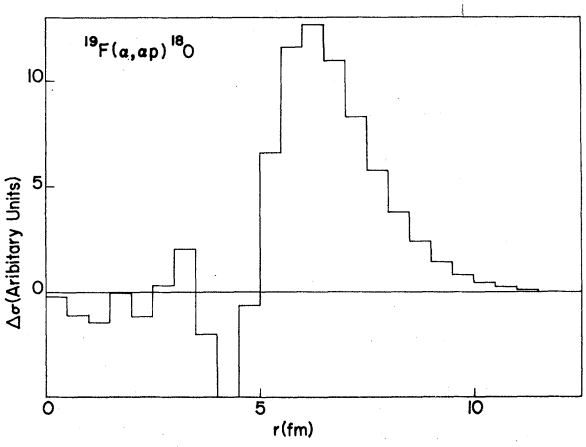

FIG. 6. Radial sensitivity of the ^{19}F$(\alpha, \alpha p)^{18}$O reaction.

C. ^{6}Li$(\alpha,\alpha p)^5$He($\frac{3}{2}^-$ resonance)

As discussed in Sec. II the energy sharing spectra for the ^{6}Li$(\alpha, \alpha p)^5$He reaction show a pronounced asymmetry about the $p_3 = 0$ point. This asymmetry arises in part from the product $(KF \times d\sigma/d\Omega|_{\alpha-p})$ in the DWIA cross section. The dependence of this product on E_α, using the final energy prescription for $d\sigma/d\Omega|_{\alpha-p}$, is shown for each angle pair in Fig. 5, and exhibits about a factor of 4 to 20 variation over the measured energy sharing spectra. However, the data, particularly the 12.5°/−27.0° angle pair, still show a pronounced asymmetry beyond that present in this factor alone.

Since the data at all three angle pairs suggest the presence of both p- and s-wave knockout, DWIA calculations were carried out for both $1p_{3/2}$ and $2s_{1/2}$ proton knockout. The bound proton wave functions were calculated by binding a proton in a Woods-Saxon well with a geometry taken from Elton and Swift[12] ($r_0 = 1.45$, $a = 0.65$) and with a binding energy corresponding to the separation energy of the centroid of the $p_{3/2}$ n-α resonance. The entrance channel optical potential was taken from an analysis[20] of 166 MeV $\alpha + {}^6$Li and for the exit channel the $\alpha + {}^5$He optical potential was obtained from an analysis[21] of 104 MeV $\alpha + {}^6$Li and the $p + {}^5$He potential from an analysis[22] of 35 MeV $p + {}^6$Li.

Since the data acquired at the 10.0°/−55.2° angle pair showed the least asymmetry, the calculations were compared primarily with them. The DWIA calculations were normalized to these data by first normalizing the $2s_{1/2}$ calculation at $p_3 = 0$ where the $1p_{3/2}$ contribution is negligible and then incoherently adding the $1p_{3/2}$ calculation normalized to obtain the best overall fit to the data. The result, along with the individual contributions, is shown in Fig. 5(a). It clearly provides a very good fit to the experimental data over the entire range. The relative normalizations are 0.1 and 0.7 for the $2s_{1/2}$ and $1p_{3/2}$ calculations, respectively. [These quantities should not be interpreted as shell-model spectroscopic factors, since a proper calculation of the overlap integral between ^{6}Li and ^{5}He requires the use of a continuum wave function for the ^{5}He $(n$-$\alpha)$ system.] The value 0.1 suggests the presence of a strong admixture of $(2s_{1/2})^2$ in the ^{6}Li ground state. Cluster model calculations give rise to this admixture in a natural way.[7,8]

DWIA calculations for the other two angle pairs using the same absolute normalizations are also shown in Figs. 5(b) and 5(c). These calculations clearly do not reproduce the asymmetry observed in the data. For the angle pair 12.0°/−47.5° they

provide a reasonable fit to the data to the left of the $p_3 = 0$ point (lower α energies), but they do not reproduce the broad peak observed at $E_\alpha \approx 115$ MeV. The disagreement between the calculation and the experimental data is even more pronounced for the 12.5°/−27.0° angle pair, but again there is reasonable agreement to the left of $p_3 = 0$.

An attempt to reconcile this discrepancy within the DWIA was made by varying the parameters in the calculation. The results of using different bound state geometries, different optical model potentials, and a different prescription (initial energy prescription) for the two-body cross section were studied. For all three angle pairs reasonable changes in the bound state geometry and optical model potentials produced no significant changes in the shape and changes of not more than 25% in the normalization of the calculated cross sections. Similarly the use of the initial energy prescription produced little change in shape and a renormalization of approximately 50% at all three angle pairs.

Presumably the asymmetry in the data arises from reaction mechanisms not included in the DWIA. A study of the kinematics of the ^{6}Li($\alpha, \alpha p$)^{5}He reaction to investigate the possibility of processes such as sequential α decay and final state interactions between outgoing pairs of particles showed no effects which would be preferentially enhanced at any particular angle pair used for this experiment. Perhaps the discrepancy arises from contributions associated with triangle graphs such as ($\alpha, 2\alpha$) followed by one of the α particles rescattering from the residual deuteron and breaking it up into a proton and neutron. However, without explicit calculation, we are unable to estimate the region of phase space populated by such a mechanism.

In conclusion, while the DWIA provides a good description of one angle pair, as well as the region of low α particle energies at the other two angle pairs, it appears that other mechanisms are important in this reaction. It is certainly possible that this problem is due to the four-body final state involved.

IV. DISCUSSION AND CONCLUSIONS

The results presented show relatively good agreement between experiment and DWIA calculations. However, it is clear that a problem exists for ^{6}Li($\alpha, \alpha p$)^{5}He, particularly when both particles go in the forward direction (12.5°/−27.0°). Whether or not this problem results from the four-body final state for this reaction requires further investigation, e.g., an examination of the ^{19}F($\alpha, \alpha p$)^{18}O reaction at other angle pairs. We plan to carry out such studies in the future.

We have shown that the ($\alpha, \alpha p$) reaction at 140 MeV is very strongly surface localized and is thus sensitive only to the asymptotic normalization of the single particle wave function. In order to compare this reaction to other knockout reactions, we have computed DWIA predictions for ($p, 2p$) and (e, ep) reactions.

In the case of ^{19}F no data exist at a suitable energy. To obtain an idea of the region of sensitivity of the various reactions we have performed DWIA calculations for $2s_{1/2}$ proton knockout via ($p, 2p$) at 150 MeV and via (e, ep) at 500 MeV, energies which are available at other accelerators. For the ($p, 2p$) calculations, optical potentials from an energy dependent analysis[23] of $p + ^{12}$C were used. For (e, ep) plane waves were assumed for the electrons and the outgoing proton wave was

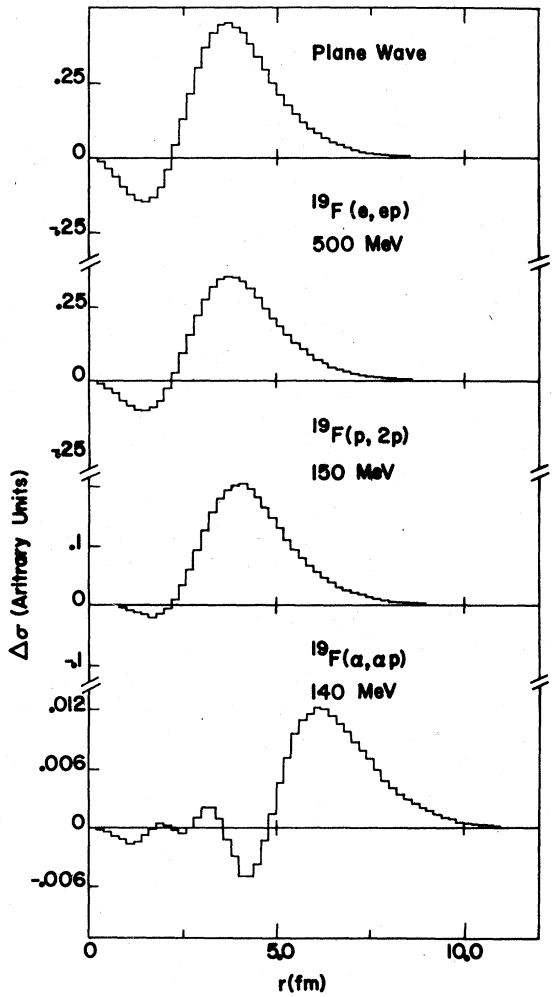

FIG. 7. Comparison of the radial sensitivities for the knockout of a $2s_{1/2}$ proton with $p_3 = 0$ for (a) plane wave (e, ep), (b) DWIA (e, ep), (c) DWIA ($p, 2p$), and (d) DWIA ($\alpha, \alpha p$) calculations.

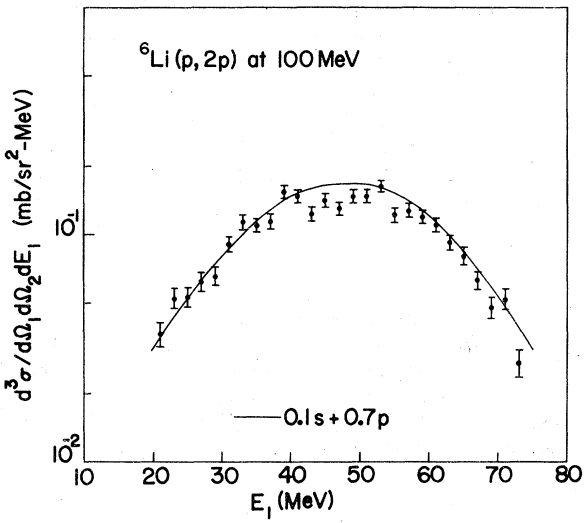

FIG. 8. The energy sharing distribution for ^{6}Li(p, $2p$)^{5}He ground state transition. The curve represents DWIA calculations with both $2s_{1/2}$ (0.1) and $1p_{3/2}$ (0.7) contributions.

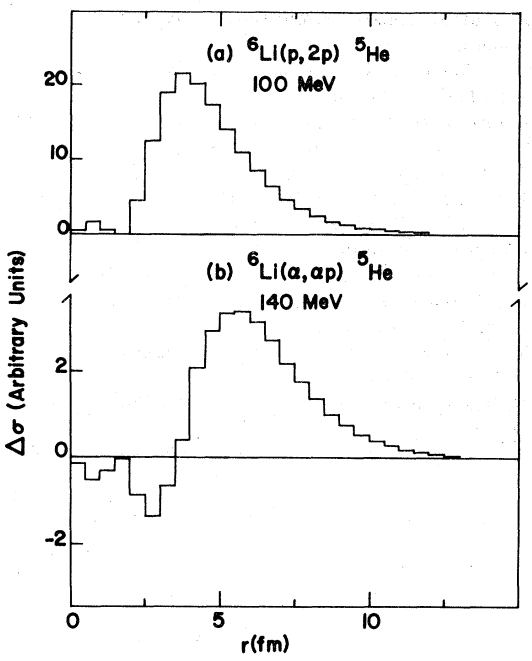

FIG. 9. The radial sensitivities for the knockout of a $2s_{1/2}$ proton with $p_3 = 0$ for the (a) ^{6}Li(p, $2p$)^{5}He, and (b) ^{6}Li(α, αp)^{5}He reactions.

distorted by the $p + ^{12}$C optical potential. The radial sensitivities at the $p_3 = 0$ points are shown in Fig. 7 for all three reactions, along with the equivalent plane wave calculation. One clearly observes the translation of the reaction into the nuclear interior as we go from (α, αp) through (p, $2p$) to (e, ep). Thus a comparison of these three reactions along with a consistent DWIA analysis should provide valuable information on the details of the nucleon single particle wave function.

We have carried out similar studies for the ^{6}Li→ ^{5}He transition. In this case data exist for both the (p, $2p$) (Ref. 8) and (e, ep) (Ref. 5) reactions. The experimental energy sharing distribution and DWIA calculations for (p, $2p$) at 100 MeV are shown in Fig. 8. The optical potentials were taken from Ref. 8. The absolute normalizations of the $1p_{3/2}$ and $2s_{1/2}$ cross sections are the same as those used for the (α, αp) reaction. The agreement with the data is remarkably good. No comparison has been made to the (e, ep) data, due to the fact that these data show inconsistencies with previous higher energy (p, $2p$) measurements.

With consistent analyses one can thus obtain excellent agreement, including the relative amounts of $1p_{3/2}$ and $2s_{1/2}$ knockout, between the (α, αp) and (p, $2p$) reactions which sample rather different regions of the nucleus. To show the regions of sensitivity for ^{6}Li we again present in Fig. 9 the $\Delta\sigma$'s at $p_3 = 0$ for these two reactions. These results are similar to those obtained for ^{19}F.

In conclusion, the (α, αp) reaction appears to be rather well described by the DWIA for angle pairs corresponding to small α-angles and relatively large p-angles (~50°). However, a more careful study of the reaction for other angle pairs is required. In addition, one would like to make a comparison with (p, $2p$) and (e, ep) for heavier nuclei such as ^{40}Ca.

The authors acknowledge the University of Maryland Computer Science Center for their generous support in providing computer time for the DWIA calculations. This research was supported in part by the National Science Foundation.

*Present address: Tsing Hua University, Taiwan, R. O. C.

[1]See G. Jacob and T. A. J. Maris, Rev. Mod. Phys. 38, 121 (1966); 45, 6 (1973) and references therein.
[2]A. N. James *et al.*, Nucl. Phys. A133, 89 (1969); A. N. James, P. T. Andrews, P. Kirkby, and B. G. Lowe, *ibid.* A138, 145 (1969).
[3]G. Landaud *et al.*, Nucl. Phys. A173, 337 (1971); S. Kullander *et al.*, *ibid.* A173, 357 (1971).
[4]J. Mougey *et al.*, Nucl. Phys. A262, 461 (1976).
[5]H. Hiramatsu *et al.*, Phys. Lett. 44B, 50 (1973); K. Nakamura *et al.*, Phys. Rev. Lett. 33, 853 (1974);

N. Izutsu, Thesis, Kyoto University, 1973 (unpublished).
[6]N. S. Chant and P. G. Roos, Phys. Rev. C 15, 57 (1977).
[7]D. R. Inglis, in *Proceedings of the Rutherford Jubilee International Conference, Manchester, 1961*, edited by J. B. Birks (Heywood, London, 1962), p. 837; Tore Berggren, G. E. Brown, and Gerhard Jacob, Phys. Lett. 1, 88 (1962); S. Saito, J. Hiura, and H. Tanaka, Prog. Theor. Phys. 39, 635 (1968).
[8]Ranjan K. Bhowmik, C. C. Chang, P. G. Roos, and H. D. Holmgren, Nucl. Phys. A226, 365 (1974); Ranjan K. Bhowmik, Ph.D. thesis, University of Maryland, 1974 (unpublished).
[9]D. I. Bonbright, Ph.D. thesis, University of Maryland, 1970 (unpublished).
[10]B. Tatischaff and I. Brissaud, Nucl. Phys. A155, 89 (1970).
[11]G. Thompson, M. B. Epstein, and Tatsuro Sawada, Nucl. Phys. A142, 576 (1970).
[12]L. R. B. Elton and A. Swift, Nucl. Phys. A94, 52 (1967).
[13]S. M. Smith *et al.*, Nucl. Phys. A207, 273 (1973).
[14]P. D. Greaves, V. Hnizdo, J. Lowe, and O. Karban, Nucl. Phys. A179, 1 (1972).
[15]G. Th. Kaschl *et al.*, Nucl. Phys. A155, 417 (1970).
[16]J. B. McGrory, Phys. Lett. 31B, 339 (1970).
[17]M. D. High *et al.*, Phys. Lett. 41B, 588 (1972).
[18]F. Perey and B. Buck, Nucl. Phys. 32, 353 (1962).
[19]P. P. Singh, P. Schwandt, and G. C. Yang, Phys. Lett. 59B, 113 (1975); G. C. Yang, Ph.D. thesis, Indiana University, 1975 (unpublished).
[20]D. Bachelier *et al.*, Nucl. Phys. A195, 361 (1972).
[21]R. M. DeVries, Jean-Luc Perrenoud, I. Slaus, and J. W. Sunier, Nucl. Phys. A178, 424 (1972).
[22]K. H. Bray *et al.*, Nucl. Phys. A189, 35 (1972).
[23]G. Igo (unpublished).